Cerebral Cortex December 2015;25:4678–4688
doi:10.1093/cercor/bhu151
Advance Access publication July 4, 2014

Disrupted Intrinsic Networks Link Amyloid-β Pathology and Impaired Cognition in Prodromal Alzheimer's Disease

Kathrin Koch[1,5,†], Nicholas E. Myers[1,5,6,†], Jens Göttler[1,5,†], Lorenzo Pasquini[1,5], Timo Grimmer[2], Stefan Förster[3,5], Andrei Manoliu[1,2,5], Julia Neitzel[1,5,7], Alexander Kurz[2], Hans Förstl[2], Valentin Riedl[1,3,5], Afra M. Wohlschläger[1,4,5], Alexander Drzezga[8,†] and Christian Sorg[1,2,3,5,†]

[1]Department of Neuroradiology, [2]Department of Psychiatry, [3]Department of Nuclear Medicine, [4]Department of Neurology, [5]TUM-Neuroimaging Center of Klinikum rechts der Isar, Technische Universität München (TUM), 81675 Munich, Germany, [6]Department of Experimental Psychology, Oxford University, Oxford OX1 3UD, UK, [7]Graduate School of Systemic Neurosciences (GSN), Ludwig-Maximilians-Universität, Biocenter, 82152 Munich, Germany and [8]Klinik und Poliklinik für Nuklearmedizin, 50937 Cologne, Germany

Address correspondence to Kathrin Koch, Department of Neuroradiology, Technische Universität München, Ismaninger Strasse 22, 81675 Munich, Germany. Email: kathrin.koch@tum.de
[†]Kathrin Koch, Nicholas E. Myers, Jens Göttler, Alexander Drzezga, and Christian Sorg equally contributed to the study.

Amyloid-β pathology (Aβ) and impaired cognition characterize Alzheimer's disease (AD); however, neural mechanisms that link Aβ-pathology with impaired cognition are incompletely understood. Large-scale intrinsic connectivity networks (ICNs) are potential candidates for this link: Aβ-pathology affects specific networks in early AD, these networks show disrupted connectivity, and they process specific cognitive functions impaired in AD, like memory or attention. We hypothesized that, in AD, regional changes of ICNs, which persist across rest- and cognitive task-states, might link Aβ-pathology with impaired cognition via impaired intrinsic connectivity. Pittsburgh compound B (PiB)-positron emission tomography reflecting in vivo Aβ-pathology, resting-state fMRI, task-fMRI, and cognitive testing were used in patients with prodromal AD and healthy controls. In patients, default mode network's (DMN) functional connectivity (FC) was reduced in the medial parietal cortex during rest relative to healthy controls, relatively increased in the same region during an attention-demanding task, and associated with patients' cognitive impairment. Local PiB-uptake correlated negatively with DMN connectivity. Importantly, corresponding results were found for the right lateral parietal region of an attentional network. Finally, structural equation modeling confirmed a direct influence of DMN resting-state FC on the association between Aβ-pathology and cognitive impairment. Data provide evidence that disrupted intrinsic network connectivity links Aβ-pathology with cognitive impairment in early AD.

Keywords: amyloid plaques, impaired cognition, intrinsic connectivity networks, PiB-PET, prodromal Alzheimer's disease, resting-state fMRI, task-fMRI

Introduction

Alzheimer's disease (AD) is the most common cause of dementia, accounting for about 60% of cases (Ferri et al. 2005). AD is characterized by progressive cell loss and deposition of neurofibrillary tangles and amyloid-β (Aβ) plaques (AP; Braak et al. 1993; Hansson et al. 2006). The Aβ hypothesis of AD suggests that abnormal cleavage of Aβ-precursor protein results in the imbalanced production and clearance of Aβ-peptides, including peptide accumulation and AP formation. Aβ-pathology, in turn, triggers neural dysfunction and degeneration (i.e., tangle formation and cell loss), finally resulting in patients' cognitive impairment (Selkoe 2002). This model raises the question of which neural mechanisms are involved in the translation of Aβ-pathology into cognitive impairments.

Intrinsic connectivity networks (ICNs) are characterized by synchronous ongoing brain activity at infra-slow frequency of about 0.1 Hz (Fox and Raichle 2007). They are functional networks, that is, the same regions, whose ongoing activity is coherent in non-task-states, largely co-activate during task-states, suggesting that intrinsic networks implement specific aspects of cognition and behavior (Smith et al. 2009; Laird et al. 2011). One explanation for this functional aspect of intrinsic networks is that functional connectivity (FC) at rest reflects the history of correlated activity changes during goal-directed behavior (Lewis et al. 2009; Berkes et al. 2011; Riedl et al. 2011).

ICNs are selectively disrupted in AD and in mild cognitive impairment (MCI), a high-risk state for AD (Gauthier et al. 2006), with the earliest disruptions occurring in default mode and attention networks (DMN and ATN; Greicius et al. 2004; Sorg et al. 2007, 2009; Agosta et al. 2012). While the DMN, which covers medial fronto-parietal areas, activates when attention is not focused on the outside world and deactivates during world-focused attention (Buckner et al. 2008), ATNs, which cover lateral fronto-parietal areas, are more active during world-focused attention and goal-directed behavior (Corbetta and Shulman 2002). We use the term ATN in line with Allen et al. (2011) referring to a couple of networks such as the dorsal or ventral ATN or lateralized central executive networks, all being located in frontal and parietal lobes (Allen et al. 2011). Aberrant resting-state FC of both DMN and ATNs overlaps and is related with Aβ-pathology in older persons with and without cognitive symptoms, suggesting a significant relationship between Aβ-pathology and network impairments (Hedden et al. 2009; Sheline et al. 2010; Drzezga et al. 2011; Mormino et al. 2011; Myers et al. 2014). Given both the cognitive relevance of intrinsic networks and the correspondence between aberrant intrinsic connectivity and Aβ-pathology, there is reason to assume that aberrant ICN FC might be a relevant mechanism linking Aβ-pathology with impaired cognition in AD.

Initial evidence for this assumption has been found for the DMN in patients and asymptomatic older adults, showing an association of increased Aβ with higher DMN activity during a memory task (Sperling et al. 2009). However, it is still unclear whether ICNs beyond the DMN show a similar correspondence between Aβ-pathology, aberrant intrinsic FC, impaired task-related activity, and impaired behavior in a task that recruits that

network. Considering that the DMN and ATNs cover regions with aberrant task-evoked activation and FC in AD dementia and MCI for a huge range of attention-demanding tasks (e.g., Dannhauser et al. 2005; Rombouts et al. 2005; Celone et al. 2006; Petrella et al. 2007; Sperling et al. 2010; Neufang et al. 2011; Mandal 2012), we hypothesized, first, spatially consistent changes in FC across both attention-demanding task- and rest-states in DMN and ATNs in AD. Regions showing such across task and rest consistent changes should be regions that are most strongly affected by the disease, and therefore potential candidates for proposed linking mechanisms via aberrant intrinsic FC. Therefore, we suggested, secondly, that these regions would link impaired network FC, Aβ-pathology, and impaired cognition in AD.

Materials and Methods

Overview

To address the study's hypotheses, we assessed patients with prodromal AD (pAD; i.e., with MCI and biological signs of AD) and healthy older adults by resting-state functional MRI (rs-fMRI) to identify ICNs, task-fMRI (i.e., an attention-demanding task with different difficulty levels) to reveal ICN changes regionally consistent for attention-relevant task- and rest-states, positron emission tomography (PET) imaging using the tracer [11C]-Pittsburgh compound B (PiB-PET) to estimate Aβ-pathology in vivo via PiB-uptake, and neuropsychological assessment to estimate general cognitive performance. Independent component analysis (ICA) of fMRI data was used to quantify the networks' FC pattern during rest and task as a surrogate measure of ICN connectivity. ICA decomposes fMRI data into statistically independent components with each component consisting of both a spatial z-map, which represents network's FC pattern across space, and a time course, which represents network's activity across time. Z-maps of rest- and task-states were the main outcome measures of the study representing FC, and were related to each other, to regional PiB-uptake, and to cognitive performance scores via pairwise correlation and structural equation modeling (SEM). The study's hypotheses were specified as follows: (i) Aberrant FC is spatially consistent across states of rest and the cognitive task in DMN and ATNs. (ii) Resting-state FC of such overlapping regions relates with both PiB-uptake and impaired cognition. Specifically, we expected resting-state FC to mediate the association between PiB-uptake and cognition.

Participants

Assessment

Twenty-four patients (10 females, age range 50–83 years) diagnosed with pAD and 16 healthy controls (9 females, age range 57–75 years) participated in the study (Table 1). All participants provided informed consent in accordance with the Human Research Committee guidelines of the Klinikum Rechts der Isar, Technische Universität, München. Patients were recruited from the Memory Clinic of the Department of Psychiatry, controls by word-of-mouth advertising. Examination of every participant included medical history, neurological examination, informant interview (Clinical Dementia Rating, CDR; Morris 1993), neuropsychological assessment (Consortium to establish a registry for AD, CERAD battery; Morris et al. 1989), structural MRI, and PiB-PET.

Table 1
Demographic and clinical–neuropsychological data

	Groups	
	Patients	Controls
N	24	16
Age	68.2 (8.4)	64.8 (5.4)
Gender (F/M)	10/14	9/7
CDR	0.5 (0)	0 (0)*
CDR-SB	1.6 (0.5)	0 (0)*
CERAD-total	66.3 (10.8)	88.1 (6.8)*

CDR: Clinical Dementia Rating; CDR-SB: CDR sum-of-the-box; CERAD: battery of the Consortium to Establish a Registry for AD; CERAD-total: summary of CERAD subtests; group comparisons: χ^2 (gender), two-sample *t*-test (age, CDR, CDR-SB, and CERAD-total).
*Significant group difference at $P < 0.05$.

Definition of pAD

pAD has been defined by the coincidence of both MCI and the presence of at least 1 of 5 supportive biological signs for AD such as medial temporal lobe atrophy or significant PiB-load (Dubois et al. 2007). Following this definition, we focused on the presence of MCI and significant PiB-uptake. MCI criteria include reported and neuropsychologically assessed cognitive impairments, largely intact activities of daily living, and excluded dementia (Gauthier et al. 2006). For significant PiB-uptake, we used a cut-off for "high" or "low" standardized uptake value (SUV) ratios of 1.15, consistent with cut-off values used in previous PiB-PET studies (Drzezga et al. 2011). Patients with high PiB binding (i.e., SUV ratio ≥1.15) were classified as PiB-positive and those with SUV ratio <1.15 were classified as PiB-negative (i.e., PiB-uptake SUV <1.15 was an inclusion criterion for healthy controls). Standardized SUV is measured for a pre-established large cortical volume of interest including lateral prefrontal, parietal, and temporal areas and the retrosplenial cortex, which are described in more detail below (see PET methods) and in Supplementary Material (Supplementary Fig. 1) (Hedden et al. 2009; Drzezga et al. 2011). One should note that our definition of pAD goes along with recent recommendations of a workgroup charged by the National Institute on Aging and the Alzheimer's Association (Albert et al. 2011), which suggested to differentiate between MCI (i.e., the presence of core clinical criteria for MCI, based on the characteristics of the clinical syndrome, and an examination of potential etiologic causes for the cognitive decline), MCI due to AD with an intermediate likelihood (i.e., the presence of core clinical criteria for MCI, either a positive biomarker reflecting Aβ deposition with an untested biomarker of neuronal injury, or a positive biomarker reflecting neuronal injury with an untested biomarker of Aβ), MCI due to AD with a high likelihood (i.e., the presence of core clinical criteria for MCI, positive biomarkers for both Aβ and neuronal injury), and MCI unlikely due to AD (i.e., negative biomarkers for both Aβ and neuronal injury).

In- and Exclusion Criteria

Patients of our study met criteria for MCI and demonstrated significant cortical PiB-uptake (PiB-positive). Healthy controls met criteria of being both without cognitive symptoms (i.e., CDR 0 and all CERAD subscores within 1 SD of age- and gender-matched performance) and PiB-negative. Exclusion criteria for entry into the study were other neurological, psychiatric, or systemic diseases (e.g., stroke, depression, and alcoholism) or clinically remarkable structural MRI (e.g., stroke lesions) potentially related to cognitive impairment. Fifteen patients/8 healthy controls were treated for hypertension (beta-blockers, ACE inhibitors, and calcium channel blockers), and 7/5 for hypercholesterolemia (statins). Two patients had diabetes mellitus, 4 received antidepressant medication (Mirtazapine and Citalopram), and no patient received cholinesterase inhibitors.

Multimodal Imaging Assessment

All participants underwent both MRI and PiB-PET imaging sessions. MRI session included structural MRI, rs-fMRI, and task-fMRI. PET and MRI sessions were conducted within 3.7 (±2.5) months for patients, and within 8 (±3.1) months for healthy controls.

Functional MRI Analysis

Resting-State Paradigm

During rs-fMRI (10 min), participants were instructed to keep their eyes closed and not to fall asleep. We verified that participants stayed awake by interrogating via intercom immediately after scanning.

Behavioral Paradigm

During task-fMRI, participants underwent an attention-demanding task with different difficulty levels (and therefore varying attention demands). We employed a visuo-motor dual-task paradigm with the aim of taxing central executive processing via orthogonal task demands (for detailed task description, please refer to Supplementary Material). By using a full factorial design with independently varying levels of difficulty in the visual and motor domains, we aimed to parametrically modulate task difficulty in a design that was still straightforward enough for patients to follow and perform at above-chance levels, even in the most difficult condition (in contrast, a more conventional task, such as typical working memory task with increasing load, could easily have brought patients to chance performance in the difficult conditions). We analyzed accuracy (ACCR) and reaction time (RT) data using a two-way mixed-effects ANOVA, with factors group (2 levels) and task difficulty (4 levels). The current analysis aims at the relationship between networks' FC during both being at rest and at an attention-demanding task state.

Data Acquisition

fMRI data were collected using a gradient-echo planar imaging sequence (echo time = 35 ms, repetition time = 2000 ms, flip angle = 82°, field of view = 220 × 220 mm², matrix = 80 × 80, 32 slices, slice thickness = 4 mm, and 0 mm interslice gap).

Data Preprocessing

For each participant, the first 3 functional scans of each fMRI session were discarded due to tissue magnetization effects. SPM5 (Wellcome Department of Cognitive Neurology, London, UK) was used for motion correction, spatial normalization into the Montreal Neurological Institute (MNI) space, and spatial smoothing with an 8 × 8 × 8 mm Gaussian kernel. To ensure data quality, particularly concerning motion-induced artifacts, point-to-point head motion was estimated for each subject (Power et al. 2012; Van Dijk et al. 2012). Excessive head motion (cumulative translation or rotation >3 mm or 3° and mean point-to-point translation or rotation >0.15 mm or 0.1°) was applied as an exclusion criterion. For rs-fMRI, none of the participants had to be excluded. For task-fMRI, 1 healthy control and 7 patients had to be removed from the analysis due to excessive movement ($n = 5$) or technical problems ($n = 3$), respectively. For both rs- and task-fMRI data, two-sample *t*-tests between groups yielded no significant results regarding translational and rotational movements of any direction ($P > 0.05$).

ICA and Measuring FC

Preprocessed data were decomposed into spatially independent components reflecting ICNs in a group-ICA framework (Calhoun et al. 2001), which is implemented in the GIFT software (http://icatb.sourceforge.net). Dimensionality estimation was performed for each individual dataset using minimum description length, resulting in a mean estimate of 35 (rs-fMRI)/59 (task-fMRI) components. For rs- and task-fMRI, data of controls and patients were concatenated and reduced by two-step principal component analysis, followed by independent component estimation with the infomax algorithm. This resulted in 2 sets of average group components for both fMRI runs, which were subsequently back-reconstructed into single-subject space. For each subject and fMRI run, each component included both a spatial map, which reflected that component's z-scored FC pattern across space, and a time course, which reflected the component's activity across time. Only spatial maps were analyzed further.

According to previous findings of aberrant medial and lateral fronto-parietal ICNs in early stages of AD (Sorg et al. 2007, 2009; Neufang et al. 2011; Agosta et al. 2012), the DMN and attentional ICNs were of interest (Allen et al. 2011). To automatically select ICNs-of-interest, we applied multiple spatial regression analyses of the 35 (rs-fMRI)/59 (task-fMRI) independent components on masks derived from a previous study (Allen et al. 2011): The anterior and posterior DMN (aDMN IC 25 and pDMN IC 53 of Allen et al. 2011), ATNs (r(ight) ATN IC 60, l (eft) ATN IC 34, and d(orsal) ATN IC 72), salience network (IC 55 of Allen et al. 2011), and the primary auditory network (IC 17 of Allen et al. 2011) as a control for the specificity of effects. Masks were generated with the WFU-Pickatlas (http://www.fmri.wfubmc.edu/). In order to evaluate consistency of selected ICNs across rest and task conditions, we created templates from identified resting-state networks in a whole group approach [$P < 0.05$, family-wise error (FWE) cluster-corrected], related these masks spatially with the 59 components of the task ICA analysis again by spatial regression as implemented in the gift toolbox, and—to foreshadow results—found consistent ICNs with respect to the above-mentioned procedure (i.e., the IC selection procedure based on templates of Allen et al. identified consistent ICNs across rest and task; for correlation coefficients see Supplementary Table 4).

Across-Subject Statistical Analysis

To statistically evaluate spatial maps of selected components, we calculated voxel-wise one-sample *t*-tests on participants' spatial z-maps for each condition and group, using SPM5 ($P < 0.05$, FWE cluster-corrected). To analyze group differences, corresponding spatial maps were entered into two-sample *t*-tests ($P < 0.05$, FWE cluster-corrected, with network volumes as covariates of no interest; for details of network volume definition see below and Supplementary material "voxel-based morphometry of structural MRI"); these two-sample *t*-tests were restricted to appropriate one-sample *t*-test masks across all participants ($P < 0.01$, uncorrected). For volumes and networks defined by overlapping group different FC for rest- and task-states (i.e., in the pDMN and rATN, see Supplementary Table 1 and Fig. 2), z-maps were averaged for each subject and condition, and compared across conditions via paired *t*-tests for each group ($P < 0.05$; restricted to subjects with both rest- and task-fMRI data).

Control Analysis for Atrophy

To control for the influence of potential atrophy on FC of networks, structural changes were estimated by the use of voxel-based morphometry (VBM) of structural MRI data, which are described in detail in Supplemental Material and elsewhere (Myers et al. 2014). In brief, by the use of VBM, images were bias-corrected, tissue classified, linearly (i.e., 12-parameter affine registration) and non-linearly (i.e., warping regularization) registered, and smoothed with a Gaussian kernel of 8 mm full-width at half maximum. Voxel-wise gray matter differences between patients and controls were examined using two-sample *t*-tests ($P < 0.05$, FWE cluster-corrected), and related with spatial patterns of aberrant FC via visual inspection. Moreover, gray matter values were extracted from those networks showing FC group differences consistent across rest and task conditions, and entered as covariates into resting-state FC group comparisons.

PiB-PET Data Analysis

To evaluate the relationship between resting-state FC and PiB-uptake, regional PiB-uptake was estimated from PiB-PET data, following previous protocols (Mosconi et al. 2008) and described in detail in Supplemental Material. In brief, after image reconstruction, correction of dead time, scatter and attenuation, SPM5 was used for image realignment, transformation into the standard stereotactic MNI space, smoothing, and statistical analysis (two-sample *t*-test, $P < 0.001$, cluster extent $k = 100$).

Relationship among Intrinsic Networks, PiB-Uptake, and Cognition

Regression Analyses

As we found spatially consistent group differences during rest and task for the pDMN and rATN in the medial and lateral posterior parietal cortex (PPC), respectively (Supplementary Table 1 and Fig. 2), the following analyses focused on these regions. Since spatial overlap of altered rest- and task-FC was small at a conservative threshold (i.e., $P < 0.05$, FWE cluster-corrected; Supplementary Table 1) but enlarged strongly at a more liberal threshold ($P < 0.05$; Fig. 2), data suggested that consistently changed FC might be underestimated (for example, ICA of across groups merged fMRI data may underestimate group differences in the FC of networks). Therefore, we decided, first, to use more liberal thresholds for unimodal group comparisons with the effect of an enlarged volume of interest of potential candidates to link Aβ-pathology with impaired cognition via intrinsic FC and, then, to combine such

enlarged volume with a complementary voxel-wise multiple regression approach to relate resting-state FC with impaired cognition/PiB-uptake in patients. The combination of volume-of-interest enlargement by liberal "entrance" thresholds and subsequent voxel-wise regression analysis is complementary, since voxel-wise approaches are sensitive for intraregional variability within enlarged volumes of interest without loss of statistical rigor. In a nutshell, our procedure increased the number of potential candidates, whose resting-state FC may relate with both Aβ-pathology and impaired cognition.

More specifically, to define an overlap region that includes all potential voxels of aberrant rest- and task-FC at high probability, we chose a liberal threshold of $P < 0.2$ for unimodal comparisons by minimizing the amount of Type II error, and defined the overlap volume by the use of MARSBAR (Brett et al. 2002). Based on this volume, voxel-wise regression analyses linking patients' rest-FC with local PiB-uptake/cognitive scores were performed. For voxel-wise regression analysis, we followed Mormino et al. (2011), who used such an approach to relate FC and PiB-uptake. For regression analyses, we used a threshold of $P < 0.05$ uncorrected with a cluster extent threshold of $k = 40$. This liberal significance threshold was chosen due to 3 reasons: (1) We tested a regionally specific hypothesis (i.e., for consistently changed FC, patients' reduced resting-state FC is related with both increased PiB-uptake and reduced cognitive performance) instead of exploratory whole-brain analysis. (2) For PiB-uptake in posterior parietal areas of pAD, liberal thresholds have to be applied as patients may show strong ceiling effects in the PiB analyses (i.e., PiB-uptake values were very high with a small intersubject variance; Engler et al. 2006; Grimmer et al. 2009). (3) The chosen threshold is similar to that of Mormino et al. (2011).

To analyze the relationship between pDMN/rATN FC at rest and local PiB-uptake, PiB-uptake scores were averaged for each overlap-region of interest (ROI). Subsequently, patients' averaged PiB-uptake scores were treated as a continuous variable and regressed voxel-wise against pDMN/rATN FC maps in SPM.

To analyze the relationship between pDMN/rATN FC and cognitive performance, we performed analogous regression analyses of pDMN/rATN spatial maps (as just described), but with regressors reflecting cognitive performance instead of PiB-uptake. To ensure consistent results, we used 2 different scores of cognitive performance. First, we used the accuracy results of the task-fMRI paradigm. More specifically, we used the error rate difference between the easiest and the most difficult conditions (ACCR 4 – ACCR 1) as a regressor to account for variance predictive of success in our particular task. Secondly, we used CERAD total scores as a regressor, reflecting general cognitive impairment (Karrasch et al. 2005).

To control for the network specificity of the reported effects, analogous analyses as described above were performed for the auditory network. To create a control-ROI correspondent to the overlap-ROI, we defined the control-ROI center by the peak of the auditory network's group difference for the resting-state condition; as a ROI radius, we defined the minimal length that enabled the spherical control ROI volume to cover given overlap-ROI volumes.

SEM Analysis

Finally, beyond pairwise voxel-wise regression analyses linking between levels of Aβ-pathology, FC, and cognition, we also investigated within one integrated analytic approach whether aberrant ICN connectivity mediates or moderates the effects of Aβ-pathology on cognition in AD. Therefore, we performed ROI-based SEM for regional PiB-uptake, intrinsic network z-maps, and cognitive scores. We extracted PiB-uptake and resting-state FC values from those regions within rATN/pDMN overlap-ROIs that showed an altered connectivity in patients compared with healthy participants (as described in Supplementary Table 1 based on two-sample *t*-tests at significance threshold $P < 0.05$, FWE cluster-corrected).

We specified 2 path models, a moderator and a mediator model. A mediator model typically consists of one (or more) independent (or exogenous) variable(s), a mediator variable, and a dependent variable. Both the independent and the mediator variables are assumed to influence the dependent variable. The independent variable influences the dependent variable both directly and indirectly, that is, through its effect on the mediating variable. Accordingly, in the present study, Aβ-pathology (i.e., PiB-uptake) constitutes the independent variable, cognitive performance (i.e., ACCR4 – ACCR1 and CERAD) the dependent variable, and FC the mediating variable. Thus, we would assume that the association between PiB-uptake and cognitive performance is mediated through the effect of PiB-uptake on FC (i.e., indirect effect).

A moderator model typically consists of one (or more) independent variable(s), a moderator variable, and a dependent variable. The major difference to the mediator model is that the moderator variable is assumed to directly influence the association between the independent and the dependent variable. Again, in the context of the present study, Aβ-pathology (i.e., PiB-uptake) constitutes the independent variable and cognitive performance (i.e., ACCR4 – ACCR1 and CERAD) the dependent variable. Assuming that FC moderates the association between Aβ-pathology and cognitive performance, we generated the moderator variable by calculating the element-wise product of PiB-uptake and FC (Baron and Kenny 1986; Schlösser et al. 2007).

SEM was performed using the program Amos 22.0.0 (http://amosdevelopment.com), applying a maximum-likelihood algorithm for estimating path coefficients. We used bootstrapping procedures which make no a priori assumptions about the distribution of the paths. The null hypothesis was tested by determining whether zero was within the 95% bias-corrected confidence intervals (CIs). The goodness-of-fit index (GFI) was used to assess the goodness-of-fit of the models.

Results

Impaired Cognition and Increased PiB-Uptake in Patients

Patients had significantly reduced CERAD total scores compared with healthy older adults (two-sample *t*-test, $P < 0.001$; Table 1). Furthermore, for the attention-demanding task of increasing difficulty during task-fMRI, two-way repeated-measures ANOVAs of accuracy ACCR and RT, with factors group (2 levels) and task difficulty (4 levels), revealed significant effects of group (ACCR $F_{1,30} = 25.4$, $P < 0.001$; RT $F_{1,30} = 16.2$, $P < 0.001$), of task difficulty (ACCR $F_{3,90} = 30.7$, $P < 0.001$; RT $F_{3,90} = 93.7$, $P < 0.001$), and a significant interaction (ACCR $F_{3,90} = 23.3$, $P < 0.001$; RT $F_{3,90} = 10.7$, $P < 0.001$). Post hoc *t*-tests revealed selective impairments of patients for the more difficult conditions, both in terms of accuracy (independent samples *t*-tests, $t_{30} = 5.51$, $P < 0.001$; $t_{30} = 0.86$, $P = 0.39$, for ACCR in the most difficult and the easiest conditions, respectively) and RTs ($t_{30} = -3.99$, $P < 0.001$; $t_{30} = -1.91$, $P = 0.07$, for RT in the most difficult and the easiest conditions, respectively; Supplementary Results and Supplementary Fig. 3 for mean accuracies and reaction times).

Patients had increased cortical PiB-uptake within the frontal, parietal, and temporal lobes compared with healthy older adults (two-sample *t*-test, $P < 0.001$ uncorrected and $k = 100$; Fig. 1*A*). The pattern of distribution corresponded well to typical findings previously described in AD (e.g., Drzezga et al. 2011).

Patients had decreased gray matter volume mainly in the temporal lobe, the anterior cingulate, and the left hippocampus (two-sample *t*-test, $P < 0.05$, FWE cluster-corrected, Supplementary Table 2 and Supplementary Fig. 4).

Posterior DMN and Right ATN FC During Rest and Task Is Consistently Disrupted in the Medial and Lateral Posterior Parietal Cortex

ICA of rest- and task-fMRI data revealed for each group spatio-temporal patterns of FC that were correspondent with the

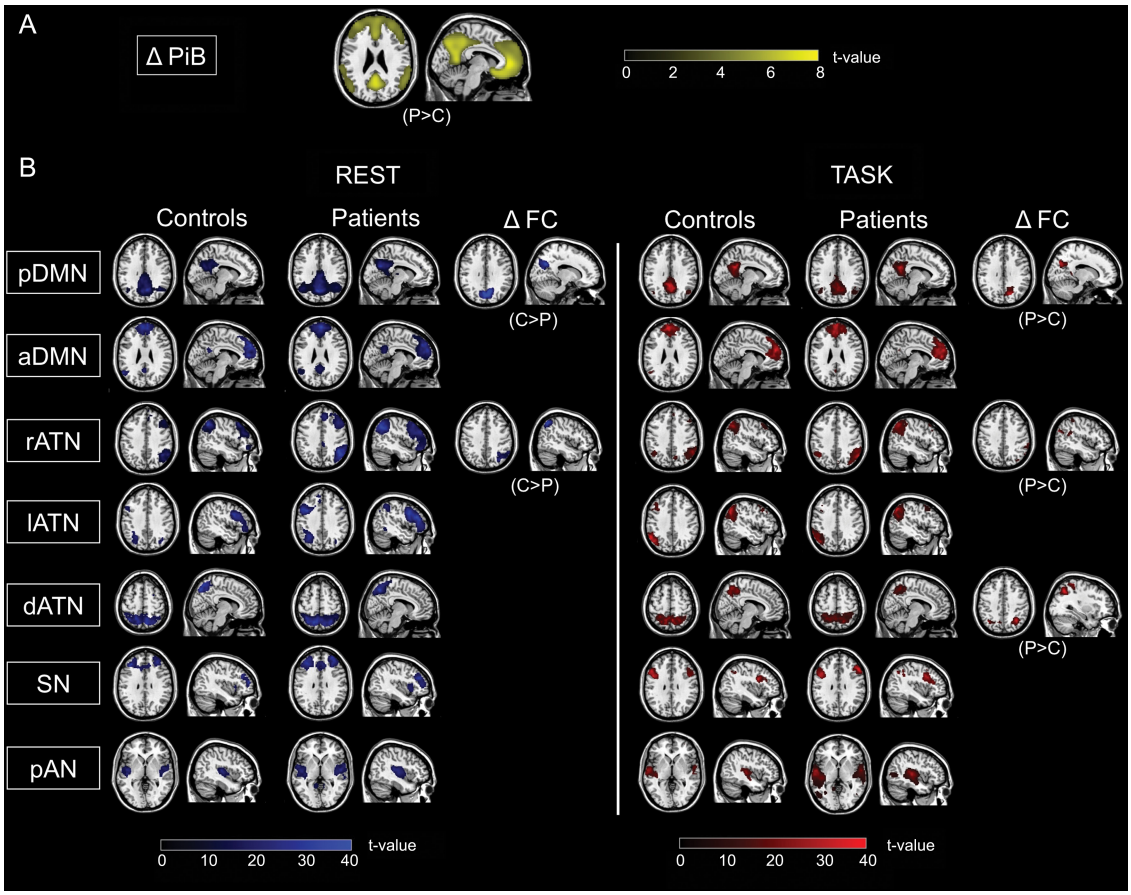

Figure 1. Multimodal imaging of patients with pAD and controls. (*A*) PiB-PET: Group difference in PiB-PET (ΔPiB) between healthy controls and patients is shown by statistical parametric map (SPM) of a two-sample *t*-test, $P < 0.001$ uncorrected, cluster extent $k = 100$; ΔPiB-uptake pattern superimposed on a single-subject high-resolution T_1 image. (*B*) Resting-state and task-fMRI: Participants' resting-state and task-fMRI data, respectively, were decomposed by ICA resulting in individual spatial maps that reflect the spatial patterns of ICNs. Columns 1–4 and 7–10: Spatial connectivity patterns of ICNs during both rest and task for patients and controls (SPMs of one-sample *t*-tests for each ICN of controls and patients; $P < 0.05$ FWE corrected at cluster level). Columns 5, 6, 11, and 12: SPMs demonstrating increased and decreased FC in patients (two-sided two-sample *t*-tests; $P < 0.05$, FWE cluster level, for visual demonstration $P < 0.05$, $k = 10$). All SPMs are projected onto a single-subject anatomical T_1-weighted image. C: healthy controls; P: patients; FC: functional connectivity; DMN: default mode network; p: posterior; a: anterior; ATN: attention network; r: right; l: left; d: dorsal; SN: salience network; pAN: primary auditory network.

posterior and anterior DMN, right, left, and dorsal ATN, salience network, and primary auditory network (Fig. 1*B*; Supplementary Table 3; one-sample *t*-test, $P < 0.05$, FWE cluster-corrected). ICNs were spatially consistent across groups (Fig. 1*B*), across tasks (Supplementary Table 4), and matched previous results (Damoiseaux et al. 2006; Sorg et al. 2007; Smith et al. 2009; Allen et al. 2011).

For the rest condition, patients had lower FC in the precuneus of the pDMN and in the inferior parietal lobule of the rATN (Fig. 1*B*; Supplementary Table 3; two-sample *t*-test, $P < 0.05$, FWE cluster-corrected). For the task condition, patients had increased FC in the precuneus of the pDMN, in the inferior parietal lobule of the rATN, and in the superior parietal cortex of the dorsal ATN (Fig. 1*B*; Supplementary Table 3; two-sample *t*-test, $P < 0.05$, FWE cluster-corrected). After correcting group differences for brain atrophy (i.e., gray matter volume), the effects in the pDMN remained significant both for the rest ($x = 6$, $y = -66$, $z = 34$, $k = 121$, $T = 4.67$, $P < 0.05$, FWE cluster-corrected) and the task condition ($x = 12$, $y = -66$, $z = 28$, $k = 83$, $T = 4.42$, $P < 0.05$, FWE cluster-corrected), while the effects in the rATN were no longer significant.

Critically, when comparing group differences for rest and task, we found overlap (i.e., aberrant FC common to both conditions) for the DMN in the precuneus (Fig. 2*A* and Supplementary Table 1) and for the rATN in the inferior parietal lobule (Fig. 2*B* and Supplementary Table 1). For such overlapping group different rest- and task-FC of the pDMN and rATN, we found lower averaged connectivity in patients and controls during rest than during task in the rATN ($P < 0.05$, Fig. 2*B*), and only for controls increased connectivity during rest than during task in the pDMN ($P < 0.05$, Fig. 2*A*).

Lower pDMN/rATN FC at Rest Correlates with Cognitive Impairment

Voxel-wise regression analyses demonstrated for the medial and lateral PPC that patients' lower pDMN/rATN FC at rest is positively correlated with patients' reduced accuracy (ACCR 4 – ACCR 1) of task performance (Fig. 3*A*,*B*; Supplementary Table 5; $P < 0.05$, uncorrected, $k = 40$). Analogous regression analyses demonstrated for the same regions that patients' decreased pDMN/rATN FC at rest is positively correlated with

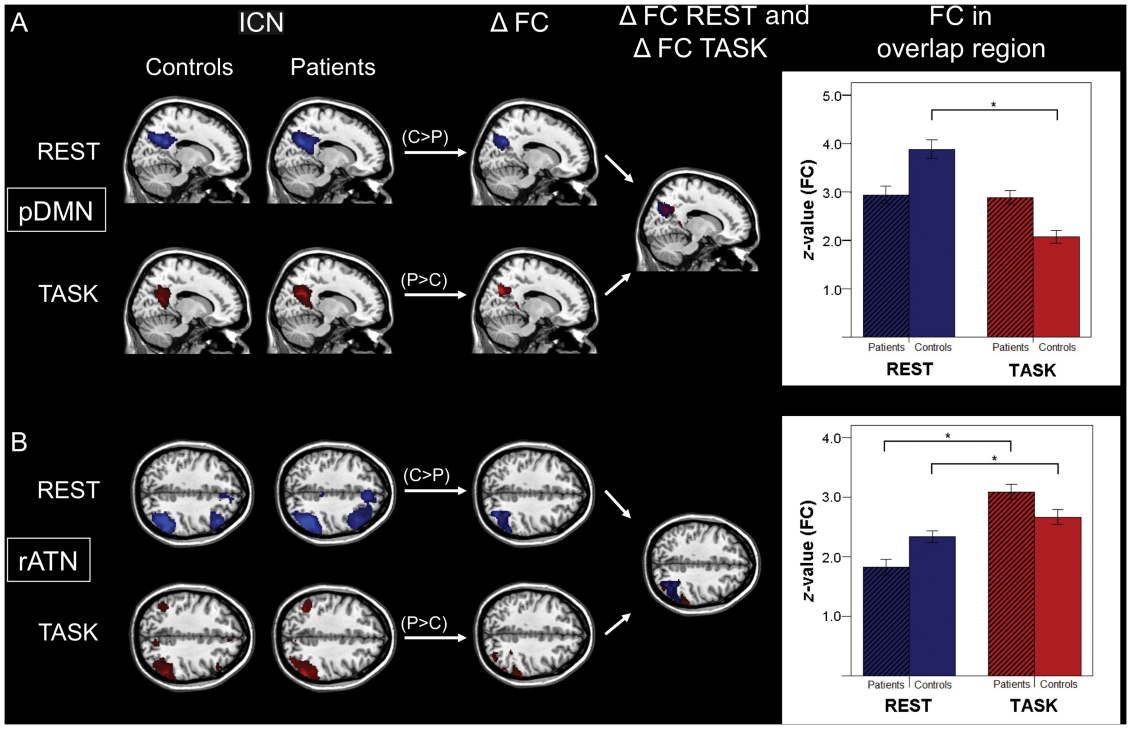

Figure 2. Spatially consistent FC changes of pDMN and rATN across rest and task in patients. Columns 1 and 2: ICNs characterized by spatial patterns of FC during rest (lines 1 and 3) and task (lines 2 and 4) concerning the pDMN (*A*) and rATN (*B*) (SPMs as in Fig. 1). Columns 3 and 4: Results of the ICN group comparisons for FC maps between patients and controls (ΔFC) for rest and task condition as well as corresponding spatial overlaps of group differences (ΔFC Rest and ΔFC Task) [SPMs with increased (P > C) and decreased (P < C) FC in patients as in Figure 1]. Right side: Bar plots representing averaged FC values for overlapping group differences for each group, condition, and ICN. Paired *t*-tests revealed FC differences across conditions ($P < 0.05$, * significant result, pDMN $T = 0.9$ (patients)/7.7 (controls); rATN $T = -7.8/-2.1$).

patients' general cognitive impairment reflected by CERAD total scores (Fig. 3*A*,*B*; Supplementary Table 5). Analogous analyses of the auditory network did not show any significant result.

Increased Local PiB-Uptake Correlates Negatively with pDMN/rATN FC at Rest

Increased PiB-uptake of patients overlapped with maps of lower FC at rest for the pDMN and rATN in the medial and lateral PPC (Fig. 4*A*,*B*). Voxel-wise regression analyses demonstrated for the medial and lateral PPC that patients' local PiB-uptake is negatively correlated with pDMN/rATN FC at rest (Fig. 4*A*,*B*; Supplementary Table 5; $P < 0.05$, uncorrected, $k = 40$). An analogous analysis of the auditory network did not show a significant result.

pDMN FC Moderates the Effects of Aβ-Pathology on Cognition

SEM revealed no significant mediating effects for pDMN and rATN with respect to Aβ-pathology and cognition. Results of the moderator analysis showed a significant negative association between pDMN PiB-uptake and cognitive (i.e., ACCR4 – ACCR1) performance ($\beta = -0.86$, $P < 0.001$) and a trend significance in terms of a positive association between pDMN FC and cognitive performance ($\beta = 0.28$, $P < 0.09$). The moderating effect of pDMN FC on the association between pDMN PiB-uptake and cognitive (i.e., ACCR4 – ACCR1) performance was significant ($\beta = -0.59$, $P < 0.001$) (Supplementary Fig. 5). The GFI of the moderator model was 0.9, indicating a good model fit. Moderating effects for the rATN and for CERAD scores were not significant.

Discussion

To address the hypothesis that, in early AD, FC of intrinsic networks is consistently changed across attention-demanding task- and rest-states, and that for such regions, aberrant intrinsic connectivity links with local Aβ-pathology and impaired cognition, patients with pAD and healthy older adults were assessed by a multimodal imaging approach including rs-fMRI and task-fMRI, PiB-PET, and neuropsychological examination. In 2 networks covering the medial and lateral PPC (namely the DMN and rATN), areas with consistently aberrant connectivity during rest and during an attention-demanding task were observed; patients' at-rest-FC of these areas was associated with both PiB-binding levels and the degree of cognitive impairment. Post hoc SEM confirmed a direct influence of DMN intrinsic connectivity on the association between PiB-uptake and cognitive impairment. Beyond the DMN, our study provides first evidence for an intrinsic network-based mechanism linking Aβ-pathology with impaired cognition in early AD.

Patients' pDMN and rATN: Consistent FC Changes During Rest and Task

Regionally Overlapping Aberrant Rest- and Task-FC

Corresponding to our first hypothesis, we observed regionally consistent abnormalities in the FC of the pDMN and rATN in patients with pAD during rest and task conditions (Figs 1

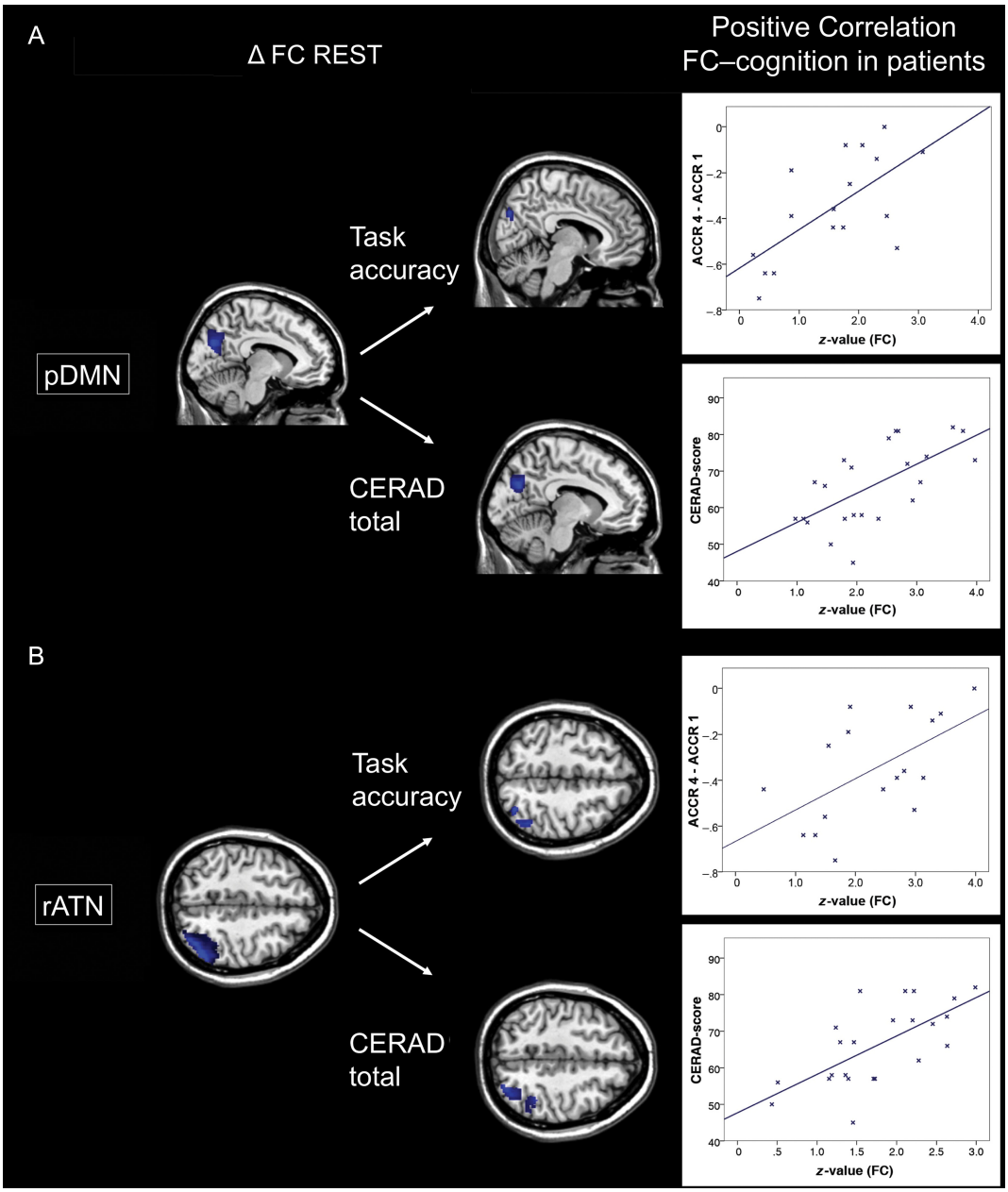

Figure 3. Patients' decreased FC of the pDMN and rATN is associated with impaired cognition. Column 1: Results of ICN group comparisons for FC maps between patients and controls (ΔFC) for the resting-state condition concerning pDMN (*A*) and rATN (*B*) (SPMs as in Fig. 1). Column 2: Patients' performance scores for cognitive accuracy (ACCR 4 – ACCR 1, assessed during task-fMRI) and CERAD total (neuropsychological assessment outside the scanner) were treated as continuous variables and regressed voxel-wise against pDMN/rATN FC maps, resulting in SPMs ($P < 0.05$ uncorrected and $k = 40$). Right side: For visualization, the relationship between cognitive performance and FC was assessed by Pearson correlation between averaged FC and cognitive performance scores across patients ($P < 0.05$; ACCR/CERAD total for pDMN $r = 0.65/0.64$, for rATN $r = 0.66/0.62$).

and 2; Supplementary Tables 1 and 3). While FC was lower during rest, it was increased during the attention-demanding task. The spatial consistency of FC group differences across rest and task suggests that pDMN/rATN intrinsic brain activity is robustly impaired in pAD (Fig. 2*A*,*B*). In the pDMN of patients, FC in the right precuneus was significantly less reduced during the task than that of healthy controls (Fig. 2*A*). This result corresponds with several previous observations of reduced DMN/medial PPC deactivation in MCI/AD during various cognitive tasks (Lustig and Buckner 2004; Rombouts et al. 2005; Petrella et al. 2007). In contrast to these studies, here we showed a reduced decrease in "connectivity" rather than in evoked activation (in line with Celone et al. 2006). In addition, increased task-FC in the right and dorsal ATN was found in the inferior and superior PPC in patients compared with controls (Figs 1*B* and 2*B*; Supplementary Table 3). Several previous studies have demonstrated increased parietal task-FC or activation, especially in MCI patients with very mild impairments (Dickerson et al. 2004; Celone et al. 2006).

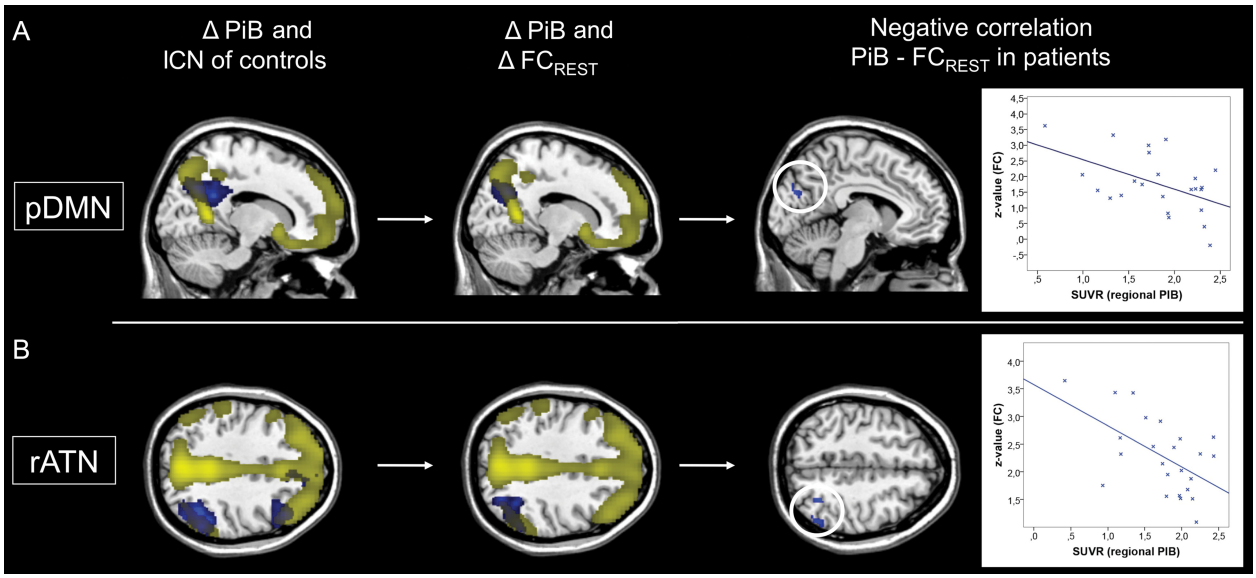

Figure 4. Patients' decreased FC of the pDMN and rATN is associated with increased local PiB-uptake. Columns 1 and 2: For the pDMN (*A*) and rATN (*B*), resting-state FC maps of controls (FC) and of group comparisons between patients and controls (ΔFC) are overlapped with the group difference map of increased PiB-uptake in patients (SPMs as in Fig. 1). Column 3: Patients' local PiB-uptake scores of overlapping rest- and task group differences were treated as continuous variables and regressed voxel-wise against pDMN and rATN FC maps, resulting in corresponding SPMs ($P < 0.05$ uncorrected and $k = 40$). Right side: For visualization, the relationship between FC and PiB-uptake was assessed by Pearson correlation between average FC and regional PiB-uptake across patients ($P < 0.05$; for pDMN $r = -0.50$, for rATN $r = -0.56$).

Directions of FC Changes

Even though the group differences in DMN and ATN connectivity were spatially consistent across rest- and task-states, the 2 networks showed dissimilar responses to the applied attention-demanding task (with the DMN barely changing in patients, while the right ATN showed an abnormal FC increase; Fig. 2). Since we have no a priori reason to believe that Aβ-pathology should affect (at least cortical) connectivity differently in different ICNs (if they are burdened with similar amounts of pathology), other factors must explain this divergence in their task response. It is well known that the amount of task-evoked FC increase in an ICN depends on the functional specialization of the ICN in question (Calhoun et al. 2001, 2008; Eichele et al. 2008; Smith et al. 2009; Laird et al. 2011; Raichle 2011). The right ATN, spanning regions known to be involved in the top-down control of attention (e.g., Nobre et al. 1997), should be functionally involved in our cognitive task including increasing top-down attention, and should therefore show a group difference that reflects the group difference in task performance. Thus, the data indicate that impaired cognitive performance goes along with an increased demand of concerted activity within task-relevant regions or networks. The abnormal connectivity increase might therefore reflect a compensatory mechanism in the presence of reduced cognitive capacities going along with pAD. On the other hand, a regular DMN decrease of FC during attention is impaired in patients.

Reduced Rest-FC and Atrophy

Concerning resting-state FC, we observed lower FC within the posterior DMN and the right ATN in the medial and lateral PPC, respectively, in patients (Fig. 1*B* and Supplementary Table 3). This result replicates a previous independent finding of our group, observed in MCI patients when compared with controls (Sorg et al. 2007). Even though atrophy was only marginally present (Supplementary Fig. 4 and Supplementary Table 2), lower FC in the DMN and rATN may have been related to reductions in gray matter volume (as previously reported, see Agosta et al. 2012). Accordingly, FC decreases in the rATN were no longer significant when adding network gray matter volumes as a covariate into the group comparisons. This indicates that findings of altered rATN connectivity in pAD are closely linked to decreases in gray matter volume. Medial and lateral components of the temporal lobes were most strongly affected by gray matter decreases (Supplementary Fig. 4 and Supplementary Table 2), but parts of the frontal lobe (predominantly orbital frontal) also showed significant gray matter decreases in patients compared with healthy controls. This finding illustrates that changes in gray matter volume should be taken into consideration when investigating alterations in FC within ATNs in patients with pAD. Of note, the strength of FC decrease in the pDMN was only reduced but remained significant after adding network gray matter volumes as a covariate into the group comparisons. While disrupted FC within the DMN is a very consistent and robust finding in MCI, AD dementia, and even in prodromal stages of the disease (Sorg et al. 2007; Hedden et al. 2009; Mormino et al. 2011; Agosta et al. 2012), disrupted FC within ATNs is less consistently reported (for example, for the dorsal ATN, see Li et al. 2011 or Sorg et al. 2007 and for lateralized ATNs, see Agosta et al. 2012 or Li et al. 2011). The obviously stronger influence of gray matter atrophy on ATN FC may explain this to some degree.

Linking PiB-Uptake, Reduced Resting-State FC, and Impaired Cognition

Patients' pDMN and rATN: Disrupted Intrinsic Connectivity Is Associated with Impaired Cognition

In patients, disrupted resting-state FC of pDMN and rATN in the medial/lateral PPC was positively related with impaired cognition (Fig. 3*A*,*B*; Supplementary Table 5). Such relationship was found for both cognitive task performance and

CERAD total scores reflecting general cognitive performance. The result is specific to the pDMN and rATN, as in the auditory network correspondent results were not found. The observed consistency across different cognitive scores suggests a general impact of disrupted pDMN/rATN connectivity in the PPC on cognitive performance. This general impact on cognitive performance might be explained by both the hub character of the medial and lateral PPC and the correspondent PPC involvement in a wide range of cognitive tasks (Gitelman et al. 1999; Corbetta and Shulman 2002; Dosenbach et al. 2008; Buckner et al. 2009; Smith et al. 2009).

Patients' pDMN and rATN: Disrupted Intrinsic Connectivity Is Associated with Local PiB-Uptake

We found that, in the medial and lateral PPC, increased local PiB uptake was overlapping and negatively correlated with patients' resting-state FC of the pDMN and rATN, respectively (Fig. 4 and Supplementary Table 5). This negative association between PiB-uptake and intrinsic FC was exactly in those areas that were characterized by both aberrant task- and at-rest-FC. This finding was specific to the pDMN and rATN, since in the auditory control network corresponding results were not found. A negative association between PiB-binding levels and resting-state FC has been reported in previous studies for the DMN (Hedden et al. 2009; Mormino et al. 2011) and the ATN (Myers et al. 2014) for persons with and without cognitive symptoms. Particularly, Drzezga et al. (2011) found that cortical regions such as precuneus or inferior parietal lobule, which are characterized by extensive FC with other parts of the cortex, are related to neuronal dysfunction (measured by FDG-PET), reduced resting-state FC, and increased PiB-uptake in patients with MCI. Taken together with results from animal studies demonstrating significant effects of local Aβ-pathology on ongoing activity (e.g., Busche et al. 2008; for a review see Palop and Mucke 2010), our data suggest that, in patients, the significant association between higher PiB-binding levels and lower intrinsic FC may reflect an adverse effect of Aβ-pathology on intrinsic FC in DMN and ATN.

No Simple Mediating Role of Aberrant Intrinsic Networks Between Amyloid Pathology and Impaired Cognition

Based on significant pairwise relations between impaired at-rest-FC and PiB-uptake/impaired cognitive performance, we expected aberrant FC to mediate between Aβ-pathology and cognition. However, instead of such a mediating effect, we found a moderating effect for only the pDMN on the relation between PiB-uptake and impaired cognitive performance for the precuneus (Supplementary Fig. 5). The higher the at-rest-FC in the precuneus, the less the effect of PiB-uptake on performance. In other words, precuneus FC works as a modulatory context factor to translate pathology effects into impaired cognition, instead of directly mediating Aβ-pathology effects. This finding suggests a complex, non-linear relationship between Aβ-pathology as defined by PiB-uptake, intrinsic FC, and cognitive performance, likely including further modulatory factors (Myers et al. 2014). We speculate that factors such as cognitive reserve (Barulli and Stern 2013) or individual baseline relationship between network connectivity and Aβ-pathology (Myers et al. 2014) might play a role. Future studies that explicitly analyze such factors are necessary.

In this context, it is important to emphasize the special role of the precuneus with respect to its PiB-uptake signal. While we found—in line with others (e.g., Hedden et al. 2009; Mormino et al. 2011)—correspondent precuneus PiB-uptake and FC reduction, suggesting a link between local plaque load and connectivity, recent neuropathological studies have challenged whether increased PiB-uptake in the precuneus really reflects increased plaque load. For example, Nelson et al. (2009) found that in patients with AD–dementia, significant precuneus plaque load was only detectable in the minority of cases. Similar findings were reported by Perez et al. (2014). Furthermore, precuneus synapse integrity seems to be largely preserved at least in early AD (Scheff et al. 2013), while cholinergic activity is specifically reduced (Ikonomovic et al. 2011). Based on these findings and on our result of linked PiB-uptake and at-rest-FC, precuneus Aβ-pathology as defined by PiB-uptake may be more strongly related to disrupted connectivity than to plaque load or aberrant synapses. Further studies are certainly necessary to better understand the specific neural underpinnings of altered PiB-uptake and Blood-oxygen-level dependent-FC measures particularly in the precuneus.

Conclusion

In pAD, we observed regionally overlapping abnormalities in FC during resting-state and cognitive task conditions in the precuneus of the posterior DMN and inferior parietal lobule of the ATN. Furthermore, patients' disrupted resting-state FC was related with both increased local PiB-uptake and impaired cognitive performance. Finally, instead of a simple linear mediation, we found disrupted DMN connectivity to have a complex moderating effect on the influence of Aβ-pathology on impaired cognition in AD.

Supplementary Material

Supplementary material can be found at: http://www.cercor.oxfordjournals.org/.

Funding

This work was supported by the Wellcome Trust (N.E.M.), Alzheimer Foundation Initiative (C.S.), German Federal Ministry of Education and Research (BMBF 01EV0710 to A.M.W. and BMBF 01ER0803 to C.S.), and the Kommission für Klinische Forschung, Technische Universität München (KKF 8765162 to C.S).

Notes

We are grateful to the participants of the study and the staff of the Department of Psychiatry and Neuroradiology for their help in recruitment and data collection. *Conflict of Interest*: All authors report no biomedical financial interests or potential conflicts of interest.

References

Agosta F, Pievani M, Geroldi C, Copetti M, Frisoni GB, Filippi M. 2012. Resting state fMRI in Alzheimer's disease: beyond the default mode network. Neurobiol Aging. 33:1564–1578.

Albert MS, DeKosky ST, Dickson D, Dubois B, Feldman HH, Fox NC, Gamst A, Holtzman DM, Jagust WJ, Petersen RC et al. 2011. The diagnosis of mild cognitive impairment due to Alzheimer's disease: recommendations from the National Institute on Aging-Alzheimer's Association workgroups on diagnostic guidelines for Alzheimer's disease. Alzheimers Dement. 7:270–279.

Allen EA, Erhardt EB, Damaraju E, Gruner W, Segall JM, Silva RF, Havlicek M, Rachakonda S, Fries J, Kalyanam R et al. 2011. A baseline for the multivariate comparison of resting-state networks. Front Syst Neurosci. 5:2.

Baron RM, Kenny DA. 1986. The moderator-mediator variable distinction in social psychological research: conceptual, strategic, and statistical considerations. J Pers Soc Psychol. 51:1173–1182.

Barulli D, Stern Y. 2013. Efficiency, capacity, compensation, maintenance, plasticity: emerging concepts in cognitive reserve. Trends Cogn Sci. 17:502–509.

Berkes P, Orbán G, Lengyel M, Fiser J. 2011. Spontaneous cortical activity reveals hallmarks of an optimal internal model of the environment. Science. 331:83–87.

Braak H, Braak E, Bohl J. 1993. Staging of Alzheimer-related cortical destruction. Eur Neurol. 33:403–408.

Brett M, Anton J-L, Valabregue R, Poline J-B. 2002. Region of interest analysis using an SPM toolbox [abstract]. Presented at the 8th International Conference on Functional Mapping of the Human Brain, 2–6 June 2002, Sendai, Japan. Available on CD-ROM in NeuroImage. 16(2).

Buckner RL, Andrews-Hanna JR, Schacter DL. 2008. The brain's default network: anatomy, function, and relevance to disease. Ann N Y Acad Sci. 1124:1–38.

Buckner RL, Sepulcre J, Talukdar T, Krienen FM, Liu H, Hedden T, Andrews-Hanna JR, Sperling RA, Johnson KA. 2009. Cortical hubs revealed by intrinsic functional connectivity: mapping, assessment of stability, and relation to Alzheimer's disease. J Neurosci. 29:1860–1873.

Busche MA, Eichhoff G, Adelsberger H, Abramowski D, Wiederhold KH, Haass C, Staufenbiel M, Konnerth A, Garaschuk O. 2008. Clusters of hyperactive neurons near amyloid plaques in a mouse model of Alzheimer's disease. Science. 321:1686–1689.

Calhoun VD, Adalı T, Pearlson GD, Pekar JJ. 2001. Spatial and temporal independent component analysis of functional MRI data containing a pair of task-related waveforms. Hum Brain Mapp. 13:43–53.

Calhoun VD, Kiehl KA, Pearlson GD. 2008. Modulation of temporally coherent brain networks estimated using ICA at rest and during cognitive tasks. Hum Brain Mapp. 29:828–838.

Celone KA, Calhoun VD, Dickerson BC, Atri A, Chua EF, Miller SL, DePeau K, Rentz DM, Selkoe DJ, Blacker D et al. 2006. Alterations in memory networks in mild cognitive impairment and Alzheimer's disease: an independent component analysis. J Neurosci. 2640:10222–10231.

Corbetta M, Shulman GL. 2002. Control of goal-directed and stimulus-driven attention in the brain. Nat Rev Neurosci. 3:215–229.

Damoiseaux JS, Rombouts SARB, Barkhof F, Scheltens P, Stam CJ, Smith SM, Beckmann CF. 2006. Consistent resting-state networks across healthy subjects. Proc Natl Acad Sci. 103:13848–13853.

Dannhauser TM, Walker Z, Stevens T, Lee L, Seal M. 2005. The functional anatomy of divided attention in amnestic mild cognitive impairment. Brain. 128:1418–1427.

Dickerson BC, Salat DH, Bates JF, Atiya M, Killiany RJ, Greve DN, Dale AM, Stern CE, Blacker D, Albert MS et al. 2004. Medial temporal lobe function and structure in mild cognitive impairment. Ann Neurol. 56:27–35.

Dosenbach NUF, Fair DA, Cohen AL, Schlaggar BL, Petersen SE. 2008. A dual-networks architecture of top-down control. Trends Cogn Sci. 12:99–105.

Drzezga A, Becker JA, Van Dijk KR, Sreenivasan A, Talukdar T, Sullivan C, Schultz AP, Sepulcre J, Putcha D, Greve D et al. 2011. Neuronal dysfunction and disconnection of cortical hubs in non-demented subjects with elevated amyloid burden. Brain. 134: 1635–1646.

Dubois B, Feldman HH, Jacova C, DeKosky ST, Barberger-Gateau P, Cummings J, Delacourte A, Galasko D, Gauthier S, Jicha G et al. 2007. Research criteria for the diagnosis of Alzheimer's disease: revising the NINCDS–ADRDA criteria. Lancet Neurol. 6:734–746.

Eichele T, Debener S, Calhoun VD, Specht K, Engel AK, Hugdahl K, von Cramon DY, Ullsperger M. 2008. Prediction of human errors by maladaptive changes in event-related brain networks. Proc Natl Acad Sci. 105:6173–6178.

Engler H, Forsberg A, Almkvist O, Blomquist G, Larsson E, Savitcheva I, Wall A, Ringheim A, Långström B, Nordberg A. 2006. Two-year follow-up of amyloid deposition in patients with Alzheimer's disease. Brain. 129:2856–2866.

Ferri CP, Prince M, Brayne C, Brodaty H, Fratiglioni L, Ganguli M, Hall K, Hasegawa K, Hendrie H, Huang Y et al. 2005. Global prevalence of dementia: a Delphi consensus study. Lancet. 366:2112–2117.

Fox MD, Raichle ME. 2007. Spontaneous fluctuations in brain activity observed with functional magnetic resonance imaging. Nat Rev Neurosci. 8:700–711.

Gauthier S, Reisberg B, Zaudig M, Petersen RC, Ritchie K, Broich K, Belleville S, Brodaty H, Bennett D, Chertkow H et al. 2006. Mild cognitive impairment. Lancet. 367:1262–1270.

Gitelman DR, Nobre AC, Parrish TB, LaBar KS, Kim Y-H, Meyer JR, Mesulam MM. 1999. A large-scale distributed network for covert spatial attention: further anatomical delineation based on stringent behavioural and cognitive controls. Brain. 122:1093–1106.

Greicius MD, Srivastava G, Reiss AL, Menon V. 2004. Default-mode network activity distinguishes Alzheimer's disease from healthy aging: evidence from functional MRI. Proc Natl Acad Sci. 101:4637–4642.

Grimmer T, Henriksen G, Wester HJ, Förstl H, Klunk WE, Mathis CA, Kurz A, Drzezga A. 2009. Clinical severity of Alzheimer's disease is associated with PIB uptake in PET. Neurobiol Aging. 30:1902–1909.

Hansson O, Zetterberg H, Buchhave P, Londos E, Blennow K, Minthon L. 2006. Association between CSF biomarkers and incipient Alzheimer's disease in patients with mild cognitive impairment: a follow-up study. Lancet Neurol. 5:228–234.

Hedden T, Van Dijk KRA, Becker JA, Mehta A, Sperling RA, Johnson KA, Buckner RL. 2009. Disruption of functional connectivity in clinically normal older adults harboring amyloid burden. J Neurosci. 29:12686–12694.

Ikonomovic MD, Klunk WE, Abrahamson EE, Wuu J, Mathis CA, Scheff SW, Mufson EJ, DeKosky ST. 2011. Precuneus amyloid burden is associated with reduced cholinergic activity in Alzheimer disease. Neurology. 77:39–47.

Karrasch M, Sinervä E, Grönholm P, Rinne J, Laine M. 2005. CERAD test performances in amnestic mild cognitive impairment and Alzheimer's disease. Acta Neurol Scand. 111:172–179.

Laird AR, Fox PM, Eickhoff SB, Turner JA, Ray KL, McKay DR, Glahn DC, Beckmann CF, Smith SM, Fox PT. 2011. Behavioral interpretations of intrinsic connectivity networks. J Cogn Neurosci. 23: 4022–4037.

Lewis CM, Baldassarre A, Committeri G, Romani GL, Corbetta M. 2009. Learning sculpts the spontaneous activity of the resting human brain. Proc Natl Acad Sci USA. 106:17558–17563.

Li R, Wu X, Fleisher AS, Reiman EM, Chen K, Yao L. 2011. Attention-related networks in Alzheimer's disease: a resting functional MRI study. Hum Brain Mapp. 33:1076–1088.

Lustig C, Buckner RL. 2004. Preserved neural correlates of priming in old age and dementia. Neuron. 42:865–875.

Mandal PK. 2012. Predictive biomarkers for Alzheimer's disease using state-of-the-art brain imaging techniques. J Alzheimer's Dis. 31: S1–S3.

Mormino EC, Smiljic A, Hayenga AO, Onami S, Greicius MD, Rabinovici GD, Janabi M, Baker SL, Yen IV, Madison CM et al. 2011. Relationships between beta-amyloid and functional connectivity in different components of the default mode network in aging. Cereb Cortex. 21:2399–2407.

Morris JC. 1993. The Clinical Dementia Rating (CDR): current version and scoring rules. Neurology. 43:2412–2414.

Morris JC, Heyman A, Mohs RC, Hughes JP. 1989. The consortium to establish a registry for Alzheimer's disease (CERAD): I. Clinical and neuropsychological assessment of Alzheimer's disease. Neurology. 39:1159–1165.

Mosconi L, Tsui WH, Herholz K, Pupi A, Drzezga A, Lucignani G, Reiman EM, Holthoff V, Kalbe E, Sorbi S et al. 2008. Multicenter standardized ^{18}F-FDG PET diagnosis of mild cognitive impairment, Alzheimer's disease, and other dementias. J Nucl Med. 49:390–398.

Myers N, Pasquini L, Göttler J, Grimmer T, Koch K, Ortner M, Neitzel J, Mühlau M, Förster S, Kurz A et al. 2014. Within-patient

correspondence of amyloid-β and intrinsic network connectivity in Alzheimer's disease. Brain. doi:10.1093/brain/awu103.
Nelson PT, Abner EL, Scheff SW, Schmitt FA, Kryscio RJ, Jicha GA, Smith CD, Patel E, Markesbery WR. 2009. Alzheimer's-type neuropathology in the precuneus is not increased relative to other areas of neocortex across a range of cognitive impairment. Neurosci Lett. 450:336–339.
Neufang S, Akhrif A, Riedl V, Förstl H, Kurz A. 2011. Disconnection of frontal and parietal areas contributes to impaired attention in very early Alzheimer's disease. J Alzheimer's Dis. 25:309–321.
Nobre AC, Sebestyen GN, Gitelman DR, Mesulam MM, Frackowiak RS, Frith CD. 1997. Functional localization of the system for visuospatial attention using positron emission tomography. Brain. 120:515–533.
Palop JJ, Mucke L. 2010. Amyloid-β-induced neuronal dysfunction in Alzheimer's disease: from synapses toward neural networks. Nat Neurosci. 13:812–818.
Perez SE, He B, Nadeem M, Wuu J, Scheff SW, Abrahamson EE, Ikonomovic MD, Mufson EJ. 2014. Resilience of precuneus neurotrophic signaling pathways despite amyloid pathology in prodromal Alzheimer's disease. Biol Psychiatry. doi:10.1016/j.biopsych.2013.12.016.
Petrella JR, Wang L, Krishnan S, Slavin MJ, Prince SE, Tran TTT, Doraiswamy PM. 2007. Cortical deactivation in mild cognitive impairment: high-field-strength functional MR imaging. Radiology. 245:224–235.
Power JD, Barnes KA, Snyder AZ, Schlaggar BL, Petersen SE. 2012. Spurious but systematic correlations in functional connectivity MRI networks arise from subject motion. NeuroImage. 59:2142–2154.
Raichle ME. 2011. The restless brain. Brain Connectivity. 1:3–12.
Riedl V, Valet M, Wöller A, Sorg C, Vogel D, Sprenger T, Boecker H, Wohlschläger AM, Tölle TR. 2011. Repeated pain induces adaptations of intrinsic brain activity to reflect past and predict future pain. NeuroImage. 57:206–213.
Rombouts SARB, Barkhof F, Goekoop R, Stam CJ, Scheltens P. 2005. Altered resting state networks in mild cognitive impairment and mild Alzheimer's disease: an fMRI study. Hum Brain Mapp. 26:231–239.
Scheff SW, Price DA, Schmitt FA, Roberts KN, Ikonomovic MD, Mufson EJ. 2013. Synapse stability in the precuneus early in the progression of Alzheimer's disease. J Alzheimers Dis. 35:599–609.
Schlösser RGM, Koch K, Wagner G. 2007. Assessing the state space of the brain with fMRI: an integrative view of current methods. Pharmacopsychiatry. 40:85–92.
Selkoe DJ. 2002. Alzheimer's disease is a synaptic failure. Science. 298:789–791.
Sheline YI, Raichle ME, Snyder AZ, Morrise JC, Head D, Wang S, Mintun MA. 2010. Amyloid plaques disrupt resting state default mode network connectivity in cognitively normal elderly. Biol Psychiatry. 67:584–587.
Smith SM, Fox PT, Miller KL, Glahn DC, Fox PM, Mackay CE, Filippini N, Watkins KE, Toro R, Laird AR et al. 2009. Correspondence of the brain's functional architecture during activation and rest. Proc Natl Acad Sci. 106:13040–13045.
Sorg C, Riedl V, Mühlau M, Calhoun VD, Eichele T, Laer L, Drzezga A, Förstl H, Kurz A, Zimmer C et al. 2007. Selective changes of resting-state networks in individuals at risk for Alzheimer's disease. Proc Natl Acad Sci. 104:18760–18765.
Sorg C, Riedl V, Perneczky R, Kurz A, Wohlschläger AM. 2009. Impact of Alzheimer's disease on the functional connectivity of spontaneous brain activity. Curr Alzheimer Res. 6:541–553.
Sperling RA, Dickerson BC, Pihlajamaki M, Vannini P, LaViolette PS, Vitolo OV, Hedden T, Becker JA, Rentz DM, Selkoe DJ et al. 2010. Functional alterations in memory networks in early Alzheimer's disease. NeuroMol Med. 12:27–43.
Sperling RA, LaViolette PS, O'Keefe K, O'Brien J, Rentz DM, Pihlajamaki M, Marshall G, Hyman BT, Selkoe DJ, Hedden T et al. 2009. Amyloid deposition is associated with impaired default network function in older persons without dementia. Neuron. 63:178–188.
Van Dijk KRA, Sabuncu MR, Buckner RL. 2012. The influence of head motion on intrinsic functional connectivity MRI. NeuroImage. 59:431–438.